Relationships Between Molecular Structure, Interfacial Structure, and Dynamics of Ionic Liquids Near Neutral and Charged Surfaces

Phwey S. Gil, Sara J. Jorgenson, Adriaan R. Riet, and D. J. Lacks*.
Department of Chemical and Biomolecular Engineering, Case Western Reserve University, Cleveland, Ohio 44106, United States

Corresponding Author
*Email: daniel.lacks@case.edu

Abstract
Room-temperature ionic liquids are being researched for a variety of applications ranging from electrochemistry, energy storage, to lubrication. In many applications with ionic liquids, key processes occur near surfaces but the impact of the complex interfacial structure of ionic liquids on its interfacial dynamics is unclear. This work uses molecular dynamics simulations to show (1) how the molecular structures of ionic liquids can affect its interfacial structure and (2) the impact of these interfacial structures on the dynamics of ionic liquids near neutral and charged surfaces. When the cation and the anion molecules are small and similar in size (e.g. *1-ethyl-3-methylimidazolium bis(trifluoromethylsulfonyl)imide*), laterally ordered structures form near neutral surfaces, and the molecules have much lower diffusivities than in the bulk. When the surfaces become charged, an order-to-disorder transition in the lateral structure increases the diffusivities. The presence of a long nonpolar tail (e.g. *1-butyl-3-methylimidazolium bis(trifluoromethylsulfonyl)imide* and *1-hexyl-3-methylimidazolium bis(trifluoromethylsulfonyl)imide*) causes the ionic liquid to be disordered near neutral surfaces, and the molecules near the surface have diffusivities only slightly lower than in the bulk. When the surfaces become charged, there is little change in the diffusivities for the systems with long nonpolar tails.

Introduction
Room-temperature ionic liquids have a unique combination of properties that make them desirable for a variety of applications, including many applications where their dynamics at interfaces with solid surfaces plays a key role. For example, their wide electrochemical windows (3-5 V near room-temperature)[1] combined with volatility and flammability lower than that for typical organic solvents[2] makes them promising for electrochemical applications, including lithium batteries[3,4]; the dynamics near interfaces with electrodes is important as the electrochemical reactions takes place at the electrode surface. Ionic liquids have also been found to be effective lubricants, both in neat form[5,6,7,8,9] and as additives[10]; lubrication, of course, is due to the dynamics of liquids at solid interfaces. An understanding of how the structure and the dynamical properties at interfaces depends on molecular structure can enable the rational design of ionic liquids that are optimized for specific applications.

The dynamics of liquids are inherently coupled to the liquid structure[11] and it is well known that ionic liquids can form a range of complex interfacial structures. Thus, it is expected that the interfacial dynamics of the ionic liquids will similarly be complex. On neutral surfaces, some experiments[12] and molecular simulations[13] have found layered structures in ionic liquids, where each layer is roughly neutral having equal numbers of cations and anions in a layer. In other cases, adsorption layers can form on neutral surfaces with either the cation or the anion exhibiting significantly higher affinity for the surface

than the other,[14, 15] creating subsequent alternating layers of anion and cation layers. On charged surfaces, experiments[16,17] and molecular simulations[18,19,20,21,22] show that ionic liquids form the type of layered structure with alternating layers of cations and anions. Ordering in the direction parallel to the surface may or may not be observed on neutral and charged surfaces, sometimes even for the same ionic liquid.[23, 24] Further subtle structural effects are suggested by the existence of long range (tens of nanometers) forces, observed in surface force apparatus[25,26] and atomic force microscopy[27] studies.

While the interfacial structures of ionic liquids have been examined in many studies, the dynamics of ionic liquids near surfaces has been the subject of fewer studies. The ionic conductivity of ionic liquids in silica nanoparticle composites is lower than in the bulk, presumably because of slower dynamics near the solid surfaces in the nanoconfined liquid.[28] A molecular dynamics study found that the diffusion coefficient of an ionic liquid near a surface is decreased in comparison to its value in the bulk,[29] while another simulation found the opposite behavior (for a different ionic liquid).[30] The one molecular dynamics simulation that we are aware of that addresses diffusion near charged walls finds that the diffusion coefficient is larger near charged walls than neutral walls.[31] Experimental studies have also probed the viscous flow behavior of ionic liquids near surfaces. The effective viscosity of ionic liquids increases by orders of magnitude when confined between surfaces.[32] The application of electrostatic potentials to surfaces confining ionic liquids can make them more lubricating or less lubricating, depending on the ionic liquid composition and the confinement distance.[33,34,35]

The dynamics of ionic liquids near surfaces are incredibly complex, and the objective of this paper is to find essential relationships between the ionic liquid molecular structure, the liquid structure, and the dynamics near neutral and charged surfaces.

Methods

Our study is based on molecular dynamics simulations, which models the system at the atomic scale and determines the trajectory of the molecules as a function of time. Key choices in applying our molecular dynamics methodology include:

(1) The role of molecular structure is addressed by systematically varying the length of the cation's hydrocarbon tail, as shown in **Figure 1**. The cations are *1-alkyl-3-methylimidazolium* molecules, where the alkyl group is an ethyl group ($[C_2MIM]^+$), a butyl group ($[C_4MIM]]^+$), or a hexyl group ($[C_6MIM]^+$). In all cases the anions are *bis(trifluoromethylsulfonyl)imide* ($[TFSI]^-$) molecules.

(2) A generic featureless surface is used rather than an atomistically detailed surface of a particular material, so that the results we see are due solely to the interactions within the ionic liquid, rather than specific liquid-surface interactions.

(3) The two surfaces are far enough apart (20 nm) so that the central region of the system is bulk-like; this simulation size enables the simulations to address behavior at a single wall, rather than the behavior of an extremely confined system where the combined influence of the two confining walls is important.

(4) The dynamics is quantified by the position-dependent lateral diffusivity (i.e., the diffusivity in the two dimensions parallel to the plane of the surface). While we only use this one measure of dynamics, we expect that other dynamic properties – e.g., ion conductivity and viscosity – will follow similarly because all dynamical properties originate from the same fundamental motions of molecules relative to each other.

The molecular dynamics simulations are carried out as follows. The bulk solution is modeled with 900 cations and 900 anions using force-fields[36,37] optimized to reproduce experimental densities, self-diffusion coefficients, and NMR rotational correlation times. Periodic boundary conditions are applied in

all directions. We first equilibrate the system at 1 bar and at the desired temperature (from 300 K to 375 K) using isothermal-isobaric simulations using the velocity-rescaling thermostat[38] with a time constant of 2 ps and the Berendsen barostat with a time constant of 4 ps.[39] Van der Waals interactions are computed directly to a cutoff of 1 nm, while Coulombic interactions are calculated with the Particle-Mesh-Ewald algorithm.[40] After equilibrating the isothermal-isobaric simulation, we simulate this system at constant volume to obtain the trajectories for analysis. The simulations are carried out with 2 fs time steps.

We then model the system with surfaces. Featureless surfaces are modeled with a generic Lennard-Jones potential of the 9-3 form to isolate the behavior of the ionic liquid from specific liquid-surface interactions. The 9-3 Lennard-Jones potential models the total interaction between particles and a diffuse solid.[41] Between the surfaces, 3600 cations and 3600 anions model the ionic liquid. We first equilibrate the system at 1 bar and at the desired temperature (from 300 K to 375 K). The simulation cell size is controlled so that it is constant at 20 nm in one direction (z), and variable in the other two directions (x, y), as shown in **Figure 2**. We carry out simulations of the system at constant volume. We also carry out simulations that include a uniform electric field that is oriented perpendicular to the surfaces (in the *z* direction); the uniform electric field generates a force on each ion proportional to the product of the ionic charge and the magnitude of the electric field. The uniform electric field is equivalent to having uniform charge densities on the surfaces. The 3DC correction is used to eliminate unphysical interactions between periodic images.[42]

GROMACS 5.1.6 software [43] is used to run the molecular dynamics simulations and Visual Molecular Dynamics[44] is used to visualize the simulations.

Results

Molecular dynamics simulations are carried out for the three ionic liquids shown in **Figure 1**, at temperatures between 300K and 375K, for the cases of bulk liquid (i.e., no surfaces), neutral surfaces, and charged surfaces with an electric field of 20 V/nm (which is equivalent to having uniform surface charge densities of ±8.85 μC/cm^2). Each simulation is run for 25 ns, which is sufficient to obtain equilibrated results.

Structure

We first address the ionic liquid structure near neutral surfaces. Results for density profiles perpendicular to neutral surfaces are shown in **Figure 3A**, where the atoms used to define the positions of the anions and the cations are shown in **Figure 1**. [C_2MIM][TFSI] has a strongly layered structure, with each layer being charge-neutral with equal numbers of cations and anions. The layering is very pronounced near the surface, and the layering persists for over two nanometers. In contrast, [C_4MIM][TFSI] and [C_6MIM][TFSI] have weaker layered structures – the peaks are much smaller and the structure disappears within about one nanometer from the surface.

The lateral structure, in the plane parallel to the neutral surface, is shown in **Figure 4**, for the single ionic liquid layer closest to the surface. These figures show a representative snapshot of this layer from the simulation, and the 2-dimensional radial distribution function (RDF) within this layer. For [C_2MIM][TFSI] on a neutral surface, this layer is highly ordered with a square-lattice structure where each ion is coordinated by four counter-ions within the layer. This high degree of ordering is evident in the RDF that displays strong peaks that persist for the entire simulation cell. The situation is very different for [C_4MIM][TFSI] and [C_6MIM][TFSI], where disorder in the structure is evident both from the snapshot of the layer and the RDF that shows no peaks beyond 1 nm.

We note in particular the special case with $[C_2MIM][TFSI]$ at 300K near neutral surfaces. The confinement by the surfaces causes this layering structure to persist through the entire system. The ionic liquid is solidified in a crystalline lattice. Within a layer, the liquid takes on a square lattice. Each adjacent layer is displaced by half of a lattice parameter, one so that two counter-ions on the adjacent layer coordinate with each ion in the original layer. While $[C_2MIM][TFSI]$ is not completely solidified at higher temperatures, the same 3-dimensional structure is observed close to the surfaces. This behavior concurs with experiments in that $[C_2MIM][TFSI]$[45] and other ionic liquids have been found experimentally to solidify on various substrates,[46] sometimes under nanoconfinement,[47,48] to form layers with thickness ranging from a few nanometers up to 50 nm.[49]

This difference in interfacial structure can be understood in terms of the nonpolar tail of the cation. Having a long nonpolar group makes the cation surfactant-like, as seen in simulations of an ionic at the liquid-vapor surface.[50] The nonpolar tail disrupts attractive interactions between the anions and the charged head groups of the cations. To maximize favorable interactions between the charged groups, the non-polar tails of the cations preferentially segregate to: (a) the surface, as evidenced by the peak closest to the surface in **Figure 3A**; and (b) to non-polar pockets within the liquid, as seen by the snapshots in **Figure 4**. A long nonpolar tail also makes the relative sizes and the shapes of the cations and the anions asymmetric – when there is size asymmetry it is harder to pack the ions into a regular lattice. These effects occur to a very small extent in $[C_2MIM]^+$, as evidenced by the very small peak in the density profile near the surface (**Figure 3A**). However, these effects are large in $[C_4MIM]^+$ and $[C_6MIM]^+$ because the non-polar tail is much longer.

We now address the liquid structure near charged surfaces. In **Figure 3B** and **Figure 3C**, we show the density profiles perpendicular to charged surfaces. In contrast to the situation near neutral surfaces, the layer nearest to a charged surface is composed exclusively of anions or cations. Moving away from the surface, the structure consists of charged layers that alternate between excess of anions and excess of cations. The liquid structures near charged surfaces are qualitatively similar for the $[C_2MIM]^+$, $[C_4MIM]^+$, and $[C_6MIM]^+$ systems; the extent of layering is again greater for the $[C_2MIM]^+$ system than for the other two systems, as seen by the layers persisting to larger separations from the surfaces.

The lateral structure of the ionic liquid in the single layer nearest the negative surface is shown in **Figure 4**, and the lateral structure for the single layer nearest the positive surface is shown in **Figure 5**. The layer nearest the negative surface is composed solely of cations, and the layer nearest the positive surface is composed solely of anions. For all three ionic liquids, these structures are disordered, as shown by the peaks in the RDF that diminish quickly towards large radii.

To summarize our results for the structure: Applying an electric field induces an order-to-disorder transition for the lateral structure of liquid near the surface for $[C_2MIM][TFSI]$, but disorder-to-disorder transitions for the lateral structures of $[C_4MIM][TFSI]$ and $[C_6MIM][TFSI]$.

Dynamics

We now address the dynamics of the molecules near surfaces. The diffusion coefficient is determined by the long-time limit of the Einstein relation,

$$\langle w^2 \rangle = 2nDt \qquad \text{(Eq. 1)}$$

where $\langle w^2 \rangle$ is the mean-squared displacement in n dimensions, t is time, and D is the diffusion coefficient. **Figure 6** shows the diffusion coefficients of the ionic liquid molecules in the lateral directions (i.e., parallel to the surfaces) as a function of position in the system; diffusivity is not well defined in the direction perpendicular to the surface because the confinement of the liquid in this dimension precludes

long-time diffusion. To take the lateral diffusion coefficient, we first partition the system into five 4 nm thick slices. For each section, we take the average lateral mean-squared displacement of the molecules that began the simulation in this slice, and we then calculate the diffusion coefficient using the Einstein relation.

First we address results for [C_2MIM][TFSI] at 350 K. Near neutral surfaces, the diffusion coefficients of [C_2MIM][TFSI] are much smaller than in the bulk-like region (in the center of the simulation cell). [C_2MIM][TFSI] dynamics are much slower near neutral surfaces because the molecules are "locked-in-place" by their neighbors, in laterally ordered structures (see **Figure 4**). In contrast, near charged surfaces, the diffusion coefficients of [C_2MIM][TFSI] are only slightly smaller than in the bulk-like region; there is little slowing of the dynamics near the walls in this case because the structure is disordered, and the molecules are not as much "locked-in-place".

For [C_4MIM][TFSI] and [C_6MIM][TFSI], the diffusion coefficients are slightly smaller near the neutral surface than in the bulk-like region. The slow-down of dynamics near the neutral surface is relatively small for these ionic liquids because they lack strong lateral order near the surface. Since the structures are disordered near both neutral and charged surfaces, the surface charge has relatively little impact on the diffusivity.

Figure 7 shows the lateral diffusion constant averaged throughout the entire system. With [C_2MIM][TFSI], charged surfaces lead to increased average lateral diffusion coefficient of the entire system at all temperatures studied (300 K to 375 K). With [C_4MIM][TFSI] and [C_6MIM][TFSI], the surface charge has no statistically significant effect on the average lateral diffusion coefficient. On neutral surfaces, the lateral structure of the layer closest to the surface is largely independent of temperature (for the temperatures studied), with [C_2MIM][TFSI] having an ordered structure that drastically slows the dynamics, and [C_4MIM][TFSI] and [C_6MIM][TFSI] having disordered structures that only slightly slows the dynamics. On charged surfaces, the structure of the layer closest to the surface is also largely independent of temperature. At low temperatures, the layered structure is more pronounced and extends further into the bulk than at high temperatures. In particular, for [C_2MIM][TFSI] at 300 K, the layered structure extends through our entire system. Thus, the coupling of the lateral order and the dynamics is unchanged throughout a wide temperature range.

Discussion

As noted in the Introduction, different types of order can occur in ionic liquids near surfaces. Order in the direction perpendicular occurs in the form of discrete layers oriented parallel to the surface. These layers can occur in two ways: (a) layers composed of roughly neutral mixtures of equal numbers of cations and anions; or (b) layers composed of mostly cations alternating with layers composed of mostly anions. Order can also occur in the directions lateral to the surface. The order that occurs depends on the molecular structure of the ions, and we have shown that long non-polar tails can inhibit lateral ordering at surfaces. Electrostatic charge on the surface can also affect the order, and our results have shown that transitions in the lateral order are brought about by changes in the surface charge. The order may also indeed depend on specific ion-surface interactions; in this study we intentionally use featureless surfaces to understand the behaviors intrinsic to the ionic liquid itself in the absence of specific interactions.

We have shown that *lateral* order near surfaces slows down the interfacial dynamics of ionic liquids. We expect this conclusion to apply to all dynamical properties, including diffusivity and ion conductivity in all directions, as well as viscosity. We quantify the dynamics in terms of the lateral diffusion coefficients because the confinement in finite space between surfaces causes the diffusivity to be not well

defined in the direction perpendicular to the surface. Nonetheless, dynamics in the direction perpendicular to the surface is coupled to the lateral dynamics, as fluid molecular motion in the lateral direction opens up opportunities for molecules to pass through in the perpendicular direction. Similarly, viscosity is a measure of the rate of stress relaxation in the system, and this stress relaxation occurs via molecular motion in all directions. Therefore, although we quantify dynamics only in terms of the lateral diffusion coefficients, we expect the conclusions about slowed dynamics to also apply to decreased ion conductivity (in all directions) and increased viscosity.

Therefore, in experimental instances where strong lateral order occurs on surfaces, we expect that this would lead to slower interfacial dynamics. For example, experiments have shown that [C_2MIM][TFSI] has high interfacial resistance (and thus low ionic conductivity) when there are neutral and laterally ordered layers on the surface.[51] The application of a high potential, led to a drastic reduction in the interfacial resistance (and increasing ionic conductivity). These experimental results can be understood in terms of the loss of the lateral order in the layers, as shown in our study. Numerous experiments have also found evidence of lateral order at ionic liquid interfaces,[52,53,54,55,56] and we predict that in these systems there will be lower interfacial diffusivity and ion conductivity, and higher interfacial viscosity.

While our study found lateral order only on neutral surfaces, experiments[57] in other systems found that lateral order can also occur at highly charged surfaces. In these cases, the ordered structures are single-component – exclusively the anion or the cation that form the layers. We expect these ordered structures to have slow dynamics as well.

Conclusion

The dynamics of ionic liquids near surfaces are relevant for many applications in electrochemistry, energy storage, and lubrication. Surfaces can induce interfacial ordering in these liquids, which depends on electrostatic and surfactant-like interactions of the polar and nonpolar moieties of the molecules. Ionic liquids with small nonpolar moieties organize more readily into ordered structures. The interfacial structure has consequences on dynamical properties, such that strong lateral order at the interface leads to slower interfacial dynamics and therefore lower interfacial diffusivity and ion conductivity and higher interfacial viscosity. While this paper specifically studied imidazolium cations with $[TFSI]^-$ anions, these general principles discussed in this paper could be applied to a broad range of ionic liquids and ionic liquid mixtures.

Acknowledgment

This material is based upon work supported by the National Science Foundation under grant numbers 1206480, 1159327 and 1659394.

Figures

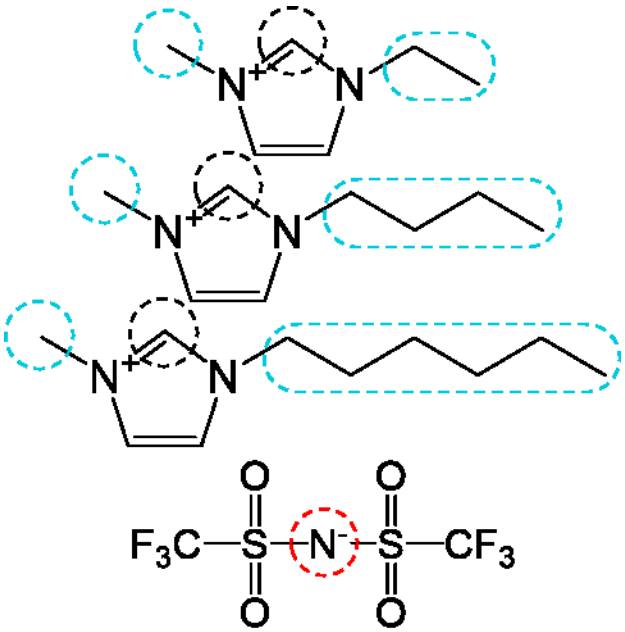

Figure 1. Chemical structures of $[C_2MIM]^+$, $[C_4MIM]^+$, $[C_6MIM]^+$, and $[TFSI]^-$. The carbon atoms circled in black and the nitrogen atom circled in red were used to define the positions of the cations and anions, respectively. All circled atoms were used to visualize the molecular dynamics trajectories.

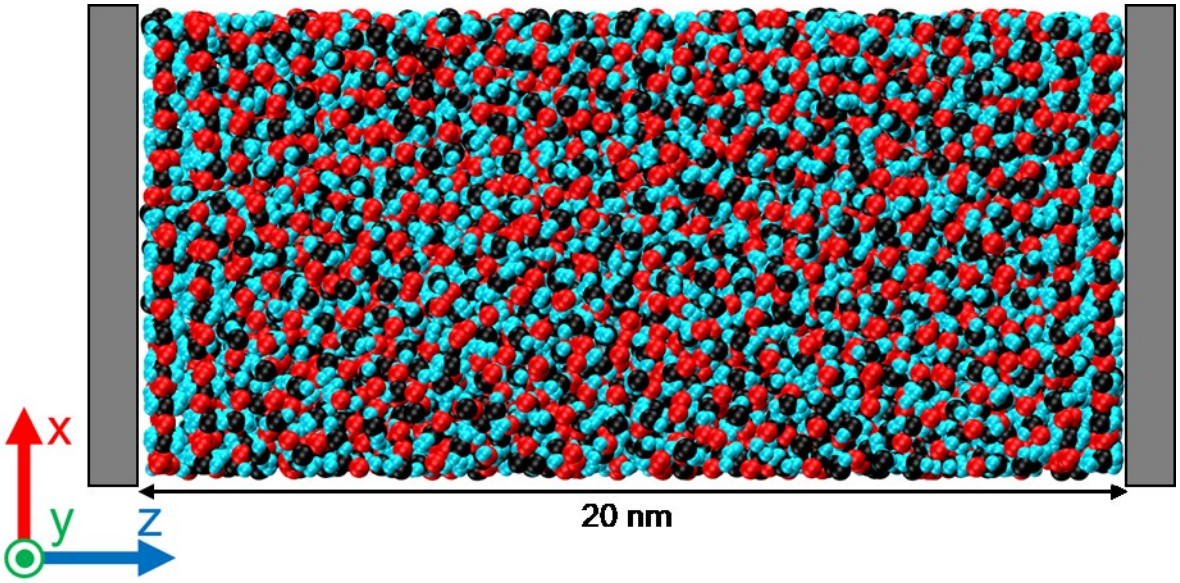

Figure 2. Molecular dynamics snapshot of $[C_2MIM][TFSI]$ at 350 K between neutral surfaces. The simulation cell is 20 nm from one surface to the other in the *z* direction, while the *x* and *y* dimensions depend on the ionic liquid and the temperature. The electric field is oriented in the *z* direction.

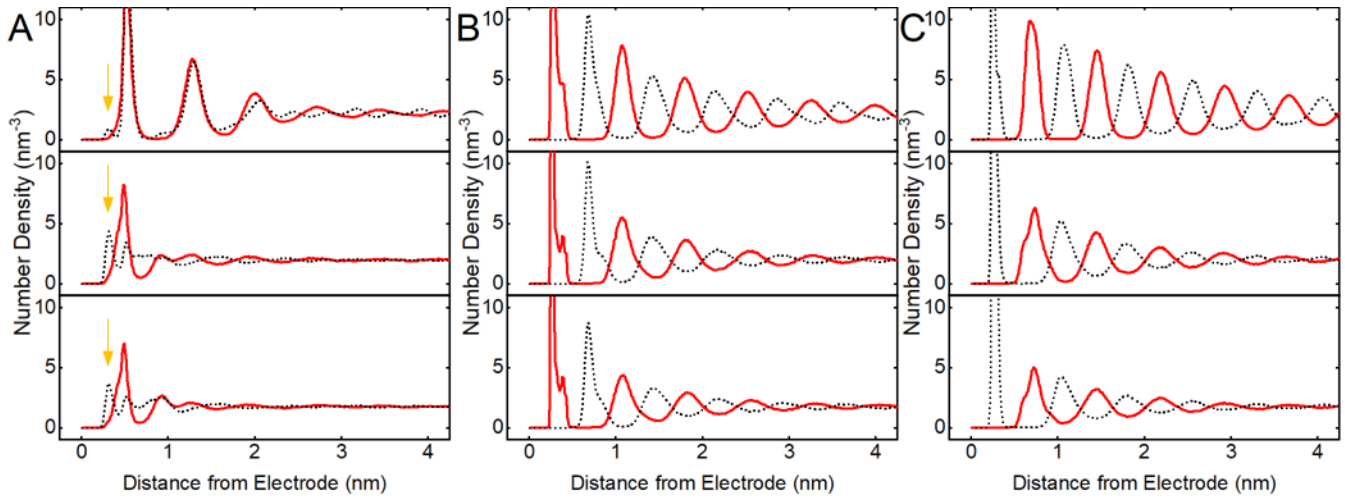

Figure 3. Number density of anions (solid red lines) and cations (dotted black lines) at 350 K near **A:** a neutral surface; **B:** a positively charged surface; and **C:** a negatively charged surface. Results shown for [C_2MIM][TFSI] (Top), [C_4MIM][TFSI] (Middle), and [C_6MIM][TFSI] (Bottom). The gold arrows point to the first cation peak near neutral surfaces.

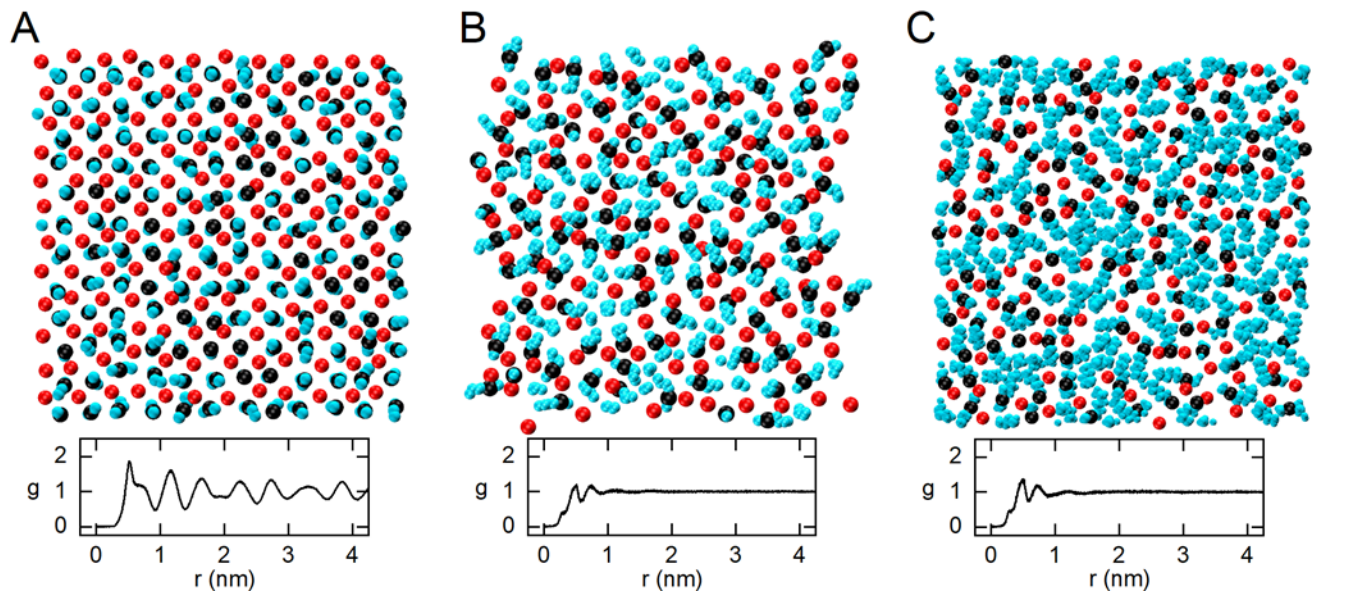

Figure 4. Molecular dynamics snapshots and lateral 2-dimensional radial distribution functions of the layer of ionic liquid nearest to a neutral surface at 350 K for **A:** [C_2MIM][TFSI], **B:** [C_4MIM][TFSI], and **C:** [C_6MIM][TFSI]. Anions are shown as red spheres, cation head groups are shown as black spheres, and the cation nonpolar tails are shown as cyan spheres. The radial distribution function is taken for the cation and anion head groups only and excludes the nonpolar groups.

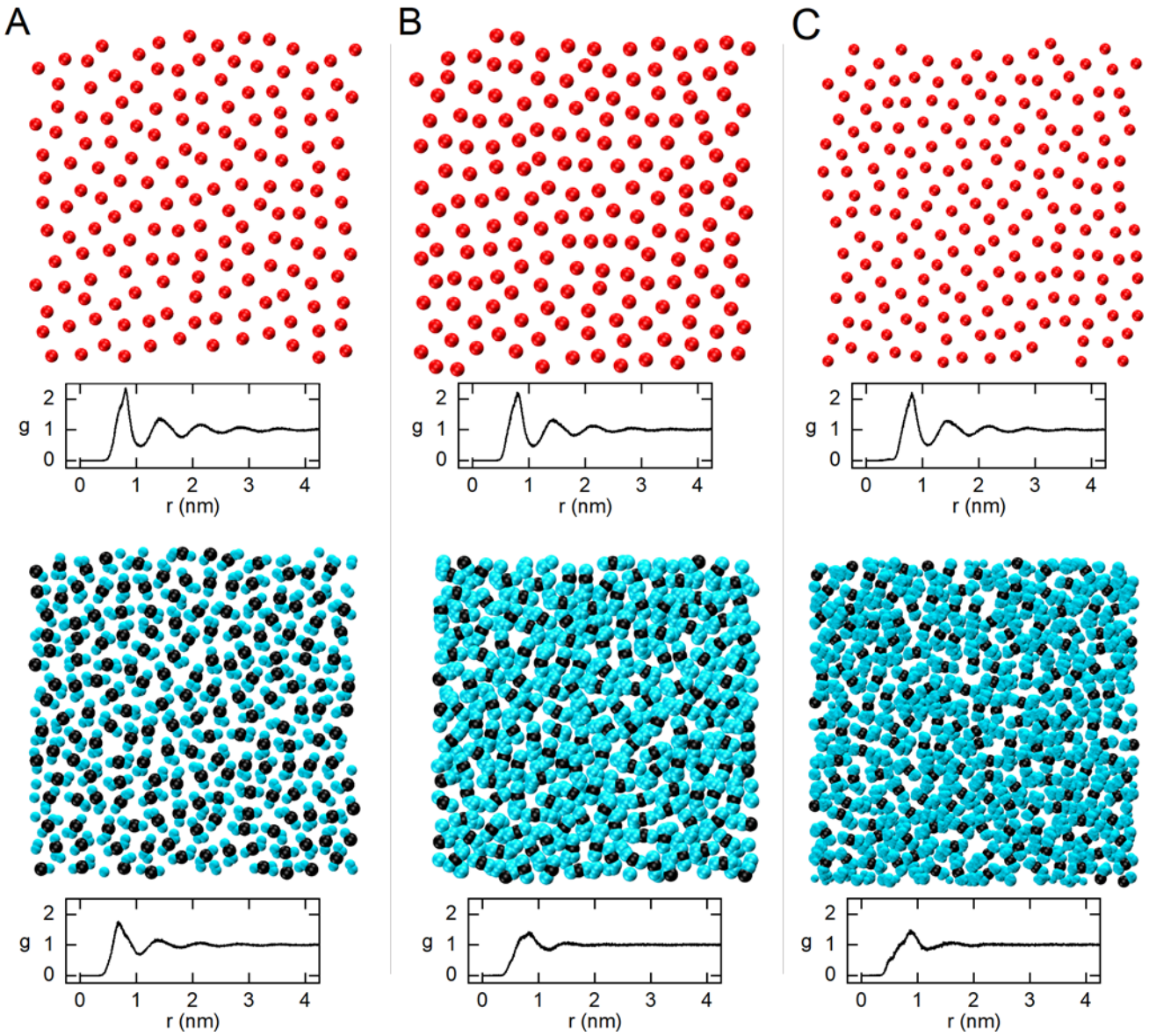

Figure 5. Molecular dynamics snapshots and lateral 2-dimensional radial distribution functions of the layer of ionic liquid at 350 K nearest to a positive surface (Top) and a negative surface (Bottom) for **A**: [C_2MIM][TFSI], **B:** [C_4MIM][TFSI], and **C:** [C_6MIM][TFSI]. Anions are shown as red spheres, cation head groups are shown as black spheres, and the cation nonpolar tails are shown as cyan spheres. The radial distribution function is taken for the cation and anion head groups only and excludes the nonpolar groups.

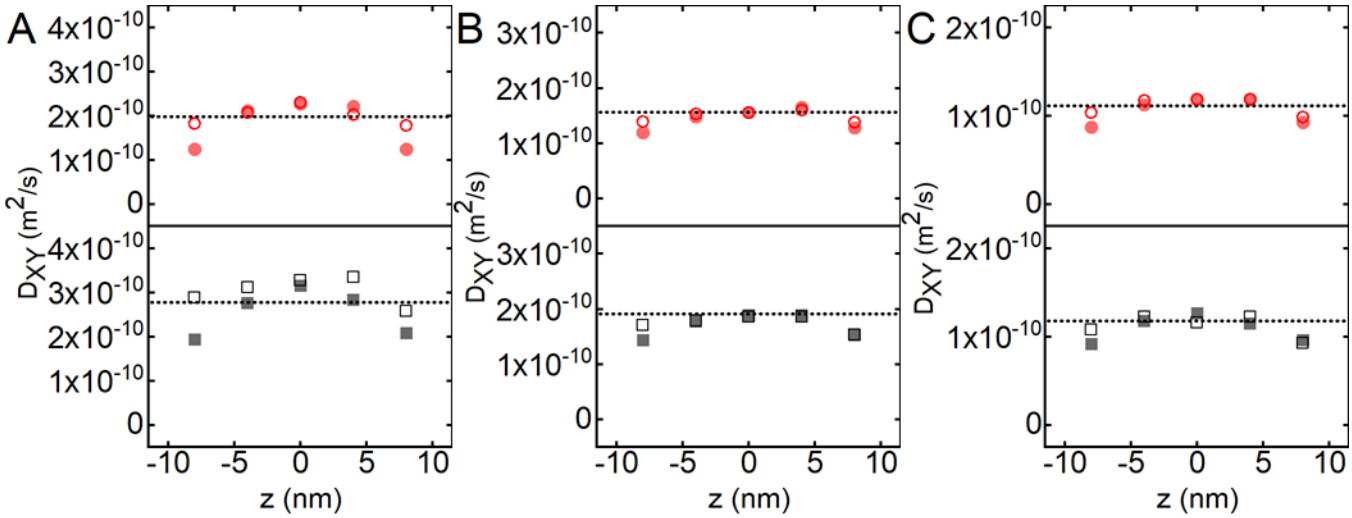

Figure 6. The lateral diffusion coefficient of ions as a function of position in the simulation cell, at 350 K. One surface is located at -10 nm, and the other surface is located at +10 nm. **A:** [C_2MIM][TFSI], **B:** [C_4MIM][TFSI], and **C:** [C_6MIM][TFSI]. With neutral surfaces, the cations are shown as solid squares and the anions are shown as solid circles. With charged surfaces (positive surface on left, negative surface on right), the cations are shown as open squares, and the anions are shown as open circles. The bulk diffusion coefficients are black dotted lines.

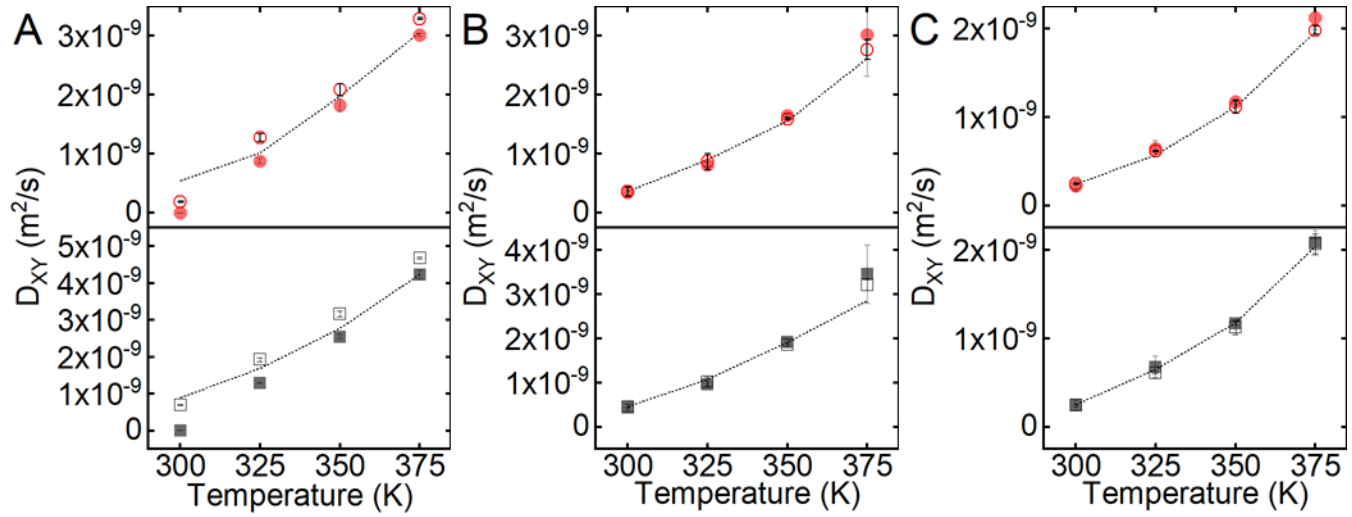

Figure 7. The average lateral diffusion coefficient of ions as a function of temperature for **A:** [C_2MIM][TFSI], **B:** [C_4MIM][TFSI], and **C:** [C_6MIM][TFSI]. With neutral surfaces, the cations are shown as solid squares and the anions are shown as solid circles. With charged surfaces, the cations are shown as solid squares, and the anions are shown as open circles. The bulk diffusion coefficients are indicated with a dotted black line.

TOC Image

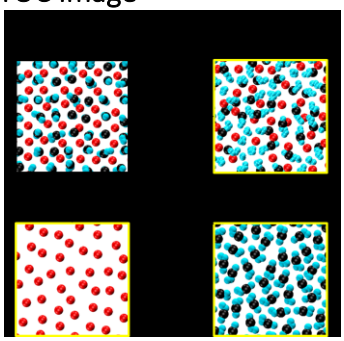

References

[1] J. Park, Y. Jung, P. Kusumah, J. Lee, K. Kwon, C. K. Lee. Application of ionic liquids in hydrometallurgy. *Int. J. Mol. Sci.* **15** 15320-15343 (2014).

[2] D. M. Fox, J. W. Gilman, A. B. Morgan, J. R. Shields, P. H. Maupin, R. E. Lyon, H. C. De Long, P. C. Trulove. Flammability and thermal analysis characterization of imidazolium-based ionic liquids. *Ind. Eng. Chem. Res.* **47** 6327-6332 (2008).

[3] M. Armand, F. Endres, D. R. MacFarlane, H. Ohno, B. Scrosati. Ionic-liquid materials for the electrochemical challenges of the future. *Nat Mater.* **8** 621-629 (2009).

[4] A. Basile, A. I. Bhatt, A. P. O'Mullane. Stabilizing lithium metal using ionic liquids for long-lived batteries. *Nat Commun.* **7:**11794 (2016).

[5] H. Xiao. Ionic liquid lubricants: Basics and applications. *Tribol. Trans.* **60** 20-30, (2017).

[6] I. Minami. Ionic liquids in tribology. *Molecules* **14** 2286-2305 (2009).

[7] F. Zhou, Y. M. Liang, W. M. Liu. Ionic liquid lubricants: Designed chemistry for engineering applications. *Chem. Soc. Rev.* **38** 2590-2599 (2009).

[8] M. Palacio, B. Bhushan. A review of ionic liquids for green molecular lubrication in nanotechnology. *Tribol. Lett.* **40** 247-268 (2010).

[9] A. E. Somers, P. C. Howlett, D. R. MacFarlane, M. A. Forsyth. A review of ionic liquid lubricants. *Lubricants* **1** 3-21 (2013).

[10] Y. Zhou, J. Qu. Ionic liquids as lubricant additives: A review. *ACS Appl. Mater. Interfaces* **9** 3209-3222 (2017).

[11] Y. Zhang, E. J. Maginn. Direct correlation between ionic liquid transport properties and ion pair lifetimes: A molecular dynamics study. *J. Phys. Chem. Lett.* **6** 700-705 (2015).

[12] R. Hayes, N. Borisenko, M. K. Tam, P. C. Howlett, F. Endres, R. Atkin. Double layer structure of ionic liquids at the Au(111) electrode interface: An atomic force microscopy investigation. *J. Phys. Chem. C* **115** 6855-6863 (2011).

[13] C. Merlet, D. T. Limmer, M. Salanne, R. van Roij, P. A. Madden, D. Chandler, B. Rotenberg. The electric double layer has a life of its own. *J. Phys. Chem. C* **118:**32 18291-18298 (2014).

[14] J. Vatamanu, O. Borodin, D. Bedrov, G. D. Smith. Molecular dynamics simulation study of the interfacial structure and differential capacitance of alkylimidazolium bis(trifluoromethanesulfonyl)imide [$C_n$mim][TFSI] ionic liquids at graphite electrodes. *J. Phys. Chem. C* **116** 7940−7951 (2012).

[15] M. H. Ghatee and F. Moosavi. Physisorption of hydrophobic and hydrophilic 1-alkyl-3-methylimidazolium ionic liquids on the graphenes. *J. Phys. Chem. C* **155** 5626-5636 (2011).

[16] J. A. Jurado, R. M. Espinosa-Marzal. Insight into the electrical double layer of an ionic liquid on graphene. *Sci. Rep* **7:**4225 (2017).

[17] S. Perkin. Ionic liquids in confined geometries. *Phys. Chem. Chem. Phys.* **14** 5052-5062 (2012).

[18] S. K. Reed, O. J. Lanning, P. A. Madden. Electrochemical interface between an ionic liquid and a model metallic electrode. *J. Chem. Phys.* **126:**084704 (2007).

[19] M. V. Fedorov, A. A. Kornyshev. Towards understanding the structure and capacitance of electric double layer in ionic liquids. *Electrochimica Acta* **53** 6835-6840 (2008).

[20] K. Kirchner, T. Kirchner, V. Ivaništšev, M. V. Fedorov. Electric double layer in ionic liquids: Structural transitions from multilayer to monolayer structure at the interface. *Electrochimica Acta* **110** 762-771 (2013).

[21] M. V. Fedorov, A. A. Kornyshev. Ionic liquid near a charged wall: Structure and capacitance of the electrical double layer. *J. Phys. Chem. B* **112**:38 11868-11872 (2008).
[22] S. Jo, S. Park, Y. Shim, Y. Jung. Effects of alkyl chain length on interfacial structure and differential capacitance in graphene supercapacitors: A molecular dynamics simulation study. *Electrochimica Acta* **247** 634-645 (2017).
[23] Y. Z. Su, Y. C. Fu, J. W. Yan, Z. B. Chen, B. W. Mao. Double layer of Au(100)/ionic liquid interface and its stability in imidazolium-based ionic liquids. *Angew. Chem. Int. Ed.* **48** 5148-5151 (2009).
[24] J. L. Ma, Q. Meng, J. Fan. Charge driven lateral structural evolution of ions in electric double layer capacitors strongly correlates with differential capacitance. *Phys. Chem. Chem. Phys.* **20** 8054-8063 (2018).
[25] M. A. Gebbie, M. Valtiner, X. Banquy, E. T. Fox, W. A. Henderson, J. N. Israelachvili. Ionic liquids behave as dilute electrolyte solutions. *PNAS* **110** 9674-9679 (2013)
[26] M. A. Gebbie, H. A. Dobbs, M. Valtiner, J. N. Israelachvili. Long-range electrostatic screening in ionic liquids. *PNAS* **112:**24 7432-7437 (2015).
[27] M. A. Gebbie et al. Long range electrostatic forces in ionic liquids. *Chem. Commum.* **53:**1214 (2017).
[28] A. Unemoto, Y. Iwai, S. Mitani, S. W. Baek, S. Ito, T. Tomai. Electrical conductivity and dynamics of quasi-solidified lithium-ion conducting ionic liquid at oxide particle surfaces. *Solid State Ionics* **201** 11-20 (2011).
[29] M. Sha, G. Wu, Y. Liu, Z. Tang, H. Fang. Drastic phase transition in ionic liquid [Dmim][Cl] confined between graphite walls: New phase formation. *J. Phys. Chem. C* **113** 4618-4622 (2009).
[30] C. Pinilla, M. G. Del Popolo, R. M. Lynden-Bell, J. Kohanoff. Structure and dynamics of a confined ionic liquid. Topics of relevance to dye-sensitized solar cells. *J. Phys. Chem. B* 109 17922-17927 (2005).
[31] N. N. Rajput, J. Monk, F. R. Hung. Structure and dynamics of an ionic liquid confined inside a charged slit graphitic nanopore. *J. Phys. Chem. C* **116** 14504-14513 (2012).
[32] M. Han, R. M. Espinosa-Marzal. Electroviscous retardation of the squeeze-out of nanoconfined ionic liquids. *J. Phys. Chem. C,* Just Accepted Manuscript (2018).
[33] H. Li, M. W. Rutland, R. Atkin. Ionic liquid lubrication: Influence of ion structure, surface potential and sliding velocity. *Phys. Chem. Chem. Phys.* **15** 14616 (2013).
[34] J. Sweeney, F. Hausen, R. Hayes, G. B. Webber, F. Endres, M. W. Rutland, R. Bennewitz, R. Atkin. Control of nanoscale friction on gold in an ionic liquid by a potential-dependent ionic lubricant layer. *Phys. Rev. Lett.* **109:**155502 (2012).
[35] L. Kong, W. Huang, X. Wang. Ionic liquid lubrication at electrified interfaces. *J. Phys. D: Appl. Phys.* **49:**225301 (2016).
[36] T. Köddermann, D. Paschek, R. Ludwig. Molecular dynamics simulations of ionic liquids: a reliable description of structure, thermodynamics, and dynamics. *Chem. Phys. Chem.* **8** 2464-2470 (2007).
[37] T. Köddermann, D. Paschek, R. Ludwig. Comparison of force fields on the basis of various model approaches – How to design the best model for the $[C_nMIM][NTf_2]$ family of ionic liquids. *Chem. Phys. Chem.* **14:**14 3368-3374 (2013).
[38] Bussi, G., Parrinello, M. Stochastic thermostats: Comparison of local and global schemes. *Comput. Phys. Commun.* **179** 26-29 (2008).
[39] H. J. C. Berendsen, J. P. M. Postma, W. F. van Gunsteren, A. DiNola, J. R. Haak. Molecular dynamics with coupling to an external bath. *J. Chem. Phys.* **81:**3684 (1984).
[40] U. Essmann, L. Perera, M. L. Berkowitz. A smooth particle mesh Ewald method. *J. Chem. Phys.* **103:**8577 (1995).

[41] W. A. Steele. The interaction of rare gas atoms with graphitized carbon black. *J. Phys. Chem.* **82**:7 817-821 (1978).
[42] I. C. Yeh and M. L. Berkowiz. Ewald summation for systems with slab geometry. *J. Chem. Phys.* **111**:3155 (1999).
[43] M. J. Abraham, T. Murtola, R. Schulz, S. Páll, J. C. Smith, B. Hess, E. Lindahl. GROMACS: High performance molecular simulations through multi-level parallelism from laptops to supercomputers. *SoftwareX* **1-2** 19-25 (2015).
[44] W. Humphrey, A. Dalke, K. Schulten. VMD: Visual molecular dynamics. *J. Mol. Graph.* **1** 33-38 (1996).
[45] S. Bovio, A. Podesta, P. Milani, P. Ballone, M. G. Del Popolo. Nanometric ionic-liquid films on silica: a joint experimental and computational study. *J. Phys. Condens. Matter* **21:**424118 (2009).
[46] Y. Yokota, T. Harada, K. Fukui. Direct observation of layered structures at ionic liquid/solid interfaces by using frequency-modulation atomic force microscopy. *Chem. Commun.* **46** 8627-8629 (2010).
[47] M. Sha, G. Wu, Y. Liu, Z. Tang, H. Fang. Drastic phase transition in ionic liquid [Dmim][Cl] confined between graphite walls: New phase formation. *J. Phys. Chem. C* **113** 4618-4622 (2009).
[48] K. Ueno, M. Kasuya, M. Watanabe, M. Mizukami, K. Kurihara. Resonance shear measurement of nanoconfined ionic liquids. *Phys. Chem. Chem. Phys.* **12** 4066-4071, (2010).
[49] J. Comtet, A. Nigues, V. Kaiser, B. Coasne, L. Bocquet, A. Siria. Nanoscale capillary freezing of ionic liquids confined between metallic interfaces and the role of electronic screening. *Nat. Materials* **16** (2017).
[50] A. S. Pensado, M. F. Costa Gomes, J. N. Canongia Lopes, P. Malfreyt, A. A. H. Padua. Effect of alkyl chain length and hydroxyl group functionalization on the surface properties of imidazolium ionic liquids. *Phys. Chem. Chem. Phys.* **13** 13518–13526 (2011).
[51] M. G. Li, L. Chen, Y. X. Zhong, Z. B. Chen, J. W. Yan, B. W. Mao. The electrochemical interface of Ag(111) in 1-ethyl-3-methylimidazolium bis(trifluoromethylsulfonyl)imide ionic liquid – A combined in-situ scanning probe microscopy and impedance study. *Electrochimica Acta* **197** 282-289 (2016).
[52] K. Fukui, Y. Yokota, A. Imanishi. Local analysis of ionic liquid/solid interfaces by frequency modulation atomic force microscopy and photoemission spectroscopy. *Chem. Rec.* **14** 964-973 (2014).
[53] M. Mezger et al. Molecular layering of fluorinated ionic liquids at a charged sapphire (0001) surface. *Science* **322** 424-428 (2008).
[54] A. J. Carmichael, C. Hardacre, J. D. Holbrey, M. Niewenhuyzen, K. R. Seddon. Molecular layering and local order in thin films of 1-alkyl-3-methylimidazolium ionic liquids using X-ray reflectivity. *Mol. Phys.* **99**:10 795-800 (2001).
[55] E. Sloutskin, B. M. Ocko, L. Tamam, I. Kuzmenko, T. Gog, M. Deutsch. Surface layering in ionic liquids: An X-ray reflectivity study. *JACS* **127** 7796-7804 (2005).
[56] H. Montes-Campos, J. M. Otero-Mato, T. Méndez-Morales, O. Cabeza, L. J. Gallego, A. Ciach, and L. M. Varela. Two-dimensional pattern formation in ionic liquids confined between graphene walls. *Phys. Chem. Chem. Phys.* **19** 24505 (2017).
[57] R. Wen, B. Rahn, O. M. Magnussen. Potential-dependent adlayer structure and dynamics at the ionic liquid/Au(111) interface: A molecular-scale in situ video-STM study. *Angew. Chem. Int. Ed.* **54** 6062-6066 (2015).